European Journal of Radiology Open 9 (2022) 100404

Contents lists available at ScienceDirect

European Journal of Radiology Open

journal homepage: www.elsevier.com/locate/ejro

Imaging of arrhythmia: Real-time cardiac magnetic resonance imaging in atrial fibrillation☆

Kerstin Laubrock [a,b,c,*], Thassilo von Loesch [c,d], Michael Steinmetz [e,f], Joachim Lotz [c,e], Jens Frahm [g], Martin Uecker [c,e,h,i], Christina Unterberg-Buchwald [b,c,e,**]

[a] Departmentof Medicine II, St. Joseph Hospital, Wüsthoffstraße 15, 12101 Berlin, Germany
[b] Department of Cardiology and Pneumology, Georg-August University, Robert-Koch-Str. 40, 37075 Goettingen, Germany
[c] Institute for Diagnostic and Interventional Radiology, Georg-AugustUniversity, Robert-Koch-Str.40, 37075 Goettingen, Germany
[d] Doctor of Internal Medicine, Elise-Averdieck-Str. 17, 27356 Rotenburg,Wuemme Germany
[e] DZHK (German Centre for Cardiovascular Research), Partner Site Goettingen, Robert-Koch-Str.40, 37075 Goettingen, Germany
[f] Department of Pediatric Cardiology and Intensive Care Medicine,Georg-August University, Robert-Koch-Str. 40, 37075 Goettingen, Germany
[g] Biomedizinische NMR, Max-Planck-Institute for Biophysical Chemistry, Am Faßberg 11, 37077 Goettingen, Germany
[h] 7170 Institute of Biomedical Imaging, GrazUniversity of Technology, Stremayrgasse16/III, 8010 Graz, Austria
[i] Cluster of Excellence "Multiscale Bioimaging:from Molecular Machines to Networks of Excitable Cells" (MBExC) University ofGöttingen, Germany

HIGHLIGHTS

- Real time cardiac magnetic imaging is superior to conventional CINE in arrhythmias: concerning image quality. Volumetric and functional analysis of real time is comparable to CINE. Acquistion time is reduced in real time. Improvement of postprocessing software of real time imaging is mandatory.

ARTICLE INFO

Keywords:
MRI
Real time
CINE
Atrial fibrillation

ABSTRACT

Objectives: Quantitative evaluations of function, volume and mass are fundamental in the diagnostic workup of different cardiovascular diseases and can be exactly determined by CMRI in sinus rhythm. This does not hold true in arrhythmia as CMR is hampered by reconstruction artifacts caused by inconsistent data from multiple heartbeats. Real-time (RT) MRI at high temporal resolution might reduce these problems.
Methods: Consecutive patients with atrial fibrillation were prospectively included and underwent RT and conventional CINE CMR in randomized order. 29 patients were studied at 1.5 T and 30 patients at 3 T. At 3 T a group of 20 subjects in sinus rhythm served as controls. RT and CINE image quality was evaluated in different planes and for different wall sections using a Likert scale (from zero to four). Volumetric analysis was performed using two types of software and differences between RT and CINE CMR were evaluated.
Results: In patients with atrial fibrillation RT CMR short axis (SA) resulted in a significantly higher image quality compared to CINE imaging both at 1.5 T and 3 T (1.5 T: mid SA: 3.55 ± 0.5 RT vs 2.6 ± 0.9 CINE, p = 0.0001; 3 T: mid SA: 3.15 ± 0.9 RT vs 2.6 ±1.0 CINE, p = 0.03); This qualitative difference was more marked and significant for the long axis views (2CV and 4CV) at 1.5 T (1.5 T: 2CV: 3.2 ± 0.6 RT vs 2.65 ± 1.1 CINE; p = 0.011; 4CV: 2.9 ± 0.69 RT vs 2.4 ± 0.9 CINE; p = 0.0044). During sinus rhythm CINE images were superior concerning diagnostic quality (3 T mid SA: 3.35 ± 0.45 RT vs 3.8 ± 0.5 CINE, p = 0.008). Quantitative analysis was successful with both software packages and the results showed a good correlation (Pearson correlation

Abbreviations: bSSFP, balanced steady-state free precession; bw, body weight; CINE, ECG-synchronized acquisition of images from multiple heartbeats covering one retrospectively sorted cardiac cycle; CMR, cardiac magnetic resonance; 2 CV, two-chamber; 4 CV, 4-chamber; ECG, electrocardiogram; ESV, end-systolic volume; EDV, end-diastolic volume; EF, ejection fraction; FOV, field of view; LV, left ventricle; NLINV, nonlinear inverse reconstruction; MM, myocardial mass; RT, real time; SA, short axis; SV, stroke volume; TE, echo time;; TR, repetition time.

☆ The work was partially supported by the German Centre for Cardiovascular Research (DZHK).

* Corresponding author at: Departmentof Medicine II, St. Joseph Hospital, Wüsthoffstraße 15, 12101 Berlin, Germany.
** Correspondence to: Christina Unterberg-Buchwald, MD, Department of Cardiology and Pneumology, University Clinic Goettingen,Robert-Koch-Str. 40, 37075 Goettingen, Germany.
E-mail address: unterberg@med.uni-goettingen.de (C. Unterberg-Buchwald).

https://doi.org/10.1016/j.ejro.2022.100404
Received 13 December 2021; Received in revised form 1 February 2022; Accepted 9 February 2022
Available online 2 March 2022

between 0.679 and 0.921 for patients). RT CMR resulted in slightly lower functional volumes than CINE CMR (3 T: patients: EDVI 86 ± 29 ml/m^2 RT vs 93 29 ml/m^2± 29 CINE, Pearson r = 0.902) but similar ejection fractions (3 T: patients: EF 47 ± 16% RT vs 45 ± 13% CINE, Pearson r = 0679; controls: EF 63 ± 6 RT vs 63 ± 3 CINE, Pearson r = 0.695).

Conclusion: RT CMR improves image quality in arrhythmic patients and renders studies more comfortable. Volumetric analysis is feasible with slightly lower values relative to CINE CMR, while ejection fractions are comparable.

1. Introduction

Quantitative evaluation of left-ventricular (LV) function is of fundamental importance in the diagnosis of different cardiovascular diseases and therefore widely used in clinical practice for prognosis and therapy guidance [1,2]. While echocardiography is still the leading modality for determination of LV function, CMR is often preferred because it is less dependent on operator experience and anatomical variations [3]. So far, CMR mostly relies on ECG-synchronized (CINE) balanced steady-state free precession (bSSFP) acquisitions that cover multiple heartbeats during repeated breath holds. Under conditions of sufficient periodicity these techniques provide excellent image quality and high blood-myocardium contrast which simplifies post-processing steps such as volumetry, determination of mass or strain analysis [4]. Unfortunately, CINE CMR is not very robust during arrhythmia, so that image quality may be severely compromised due to multiple ectopic beats or atrial fibrillation or excessive respiratory motion [5]. In the past decade several approaches for accelerated CMR acquisitions have been proposed which commonly employ data undersampling schemes in combination with iterative image reconstructions based on compressed sensing or other advanced parallel imaging methods, for example see [6–9].

In particular, recent advances in nonlinear inverse reconstruction (NLINV) now offer continuous recordings of high-quality images in real time, i.e. at high temporal resolution during free breathing and independent of ECG-synchronization [10–12]. Thus, real-time MRI emerges as a promising alternative for CMR of patients with arrhythmia. In the present work, we acquired real-time movies of 59 patients with atrial fibrillation and 20 controls at 33 ms resolution using a highly undersampled radial bSSFP sequence with NLINV reconstruction. We compared image quality and functional analyses in patients with sinus rhythm and atrial fibrillation to acquisitions with standard CINE imaging.

2. Methods

2.1. Study population

The study cohort consists of patients with atrial fibrillation (30 patients were investigated by CMR at 1.5 T (Symphony, Siemens Healthineers, Germany) and 29 patients at 3 T (Skyra, Siemens Healthineers, Germany). A group of 20 control subjects with sinus rhythm was scanned at 3 T. For demographic details see Table 1.

Table 1
Demographics of study cohort.

Demographics	Controls 3 T	Patients 3 T	Patients 1.5 T
Population (n)	20	29	30
Gender (f/m)	12/8	8/21	11/19
Age (years)	26.5 ± 3.2 (21 – 34)	68.0 ± 12.8 (38 – 84)	68.9 ± 9.1 (50 – 91)
BMI (kg/m^2)	22.4 ± 4.7	29.1 ± 2.1	27.0 ± 4.6
mean HF (min, max) [beats/min]	62.1 (51 – 82)	76.6 (59 – 101)	56.2 (47–116)

Data are given as mean ± standard deviation, age is expressed as mean and (range).

Patients and controls were consecutively and prospectively included. They all had to be in 12-lead ECG-proved atrial fibrillation or sinus rhythm immediately before the CMR. All subjects gave written informed consent before each CMR examination. The study was approved by the local ethics committee.

2.2. Cardiovascular magnetic resonance acquisition

Patients and controls underwent CMR in supine position using an 8-channel (1.5 T) and 18-channel (3 T) cardiac array coil. ECG-gated bSSFP CINE acquisitions with GRAPPA acceleration factor of 2 were carried out during multiple brief periods of breath-holding and arrhythmia rejection during CINE.

Operators were blinded to review of the scans during the scanning session.

The method resulted in retrospectively sorted cardiac cycles with 25 phases. RT CMR was performed using highly undersampled radial bSSFP sequences with NLINV reconstruction as described [13]. The order of RT and CINE CMR was randomized. Typical CMR parameters are given in Table 2. For quality scoring and functional analysis resting-state RT and CINE images were obtained in short-axis (SA) orientation covering the whole left ventricle from base to apex as well as in 2-chamber (2 C) and 4-chamber (4 C) views.

2.3. Image evaluation

Image quality was determined blinded and independently by two observers (each with more than four years experience in daily CMR appraisal. Image quality was scored on a modified Likert scale [14] ranging from 0 = no diagnostic quality to 1 = reduced diagnostic quality, 2 = diagnostic quality with many artifacts, 3 = good diagnostic quality with some artifacts, and 4 = optimal diagnostic quality. Criteria involved overall image quality concerning diagnostic value, noise, and artifacts (bSSFP banding, radial streaking, motion). In SA views sharpness of the endocardial borders and the papillary muscles was assessed. Scoring was repeated after 3 months for all 1.5 T images as well as for 6/29 patients and 5/20 controls of the 3 T cohort by the same observers.

Table 2
Acquisition parameters for RT and CINE CMR.

	1.5 T		3 T	
	CINE	RT	CINE	RT
Number of images	25	344	25	80–600
Slice thickness [mm]	8	8	6	6
Field-of view [mm^2]	380 × 285[a]	256 × 256	380 × 256[a]	256 × 256
Matrix size [pixel]	256 × 192[a]	144 × 144	256 × 192[a]	160 × 160
Spatial resolution [mm^3]	1.5 × 1.5	1.8 × 1.8	1.3 × 1.3	1.6 × 1.6
Flip angle [degree]	64°	55°[a]	53°	30°[a]
Echo time [ms]	1.36	1.54	1.51	1.28
Temporal resolution [ms]	38.4[a] (16.6 – 62.2)	40.7	41.4[a] (16.56 – 62.2)	33

[a] Adapted if necessary

2.4. Functional analysis

CINE CMR SA datasets were analyzed using the commercially available software QMass (Medis Suite version 2.1.12.6., Medis, Leiden, The Netherlands). Contours were placed around endocardial and epicardial LV borders on all image slices in end-diastole and end-systole that contained 50% or more full-thickness myocardium. The sums of the traced volumes in end-diastolic (ED) and end-systolic (ES) images were used to calculate ED volume (EDV) and ES volume (ESV) using a disc summation technique [15]. EDV and ESV were then used to calculate stroke volume (SV), ejection fraction (EF) and LV mass. Papillary muscles were included in the LV mass if visually indistinguishable from the myocardial wall, but otherwise assigned to the LV blood pool. Segmentation was performed semi-automatically and corrected manually as recommended [16].

RT CMR SA stacks were analyzed using two different software tools. RT images at 1.5 T were acquired for 20 s and consisted of 300–400 consecutive frames per plane (depending on the heart rate). Segmentation for this sub-group was performed using QMass software as demonstrated in Fig. 1. ED and ES images were selected by visual inspection (widest and smallest diameter). Starting with the third ED interval 7 consecutive heart beats were extracted and manually segmented for the entire 7 SA stacks. Afterwards mean values of the 7 heart beats (that means 7 entire SA stacks) were computed. The duration of each heart beat was calculated by multiplying the number of frames per beat with the acquisition time (33 ms). As no ECG-trigger signal was stored in the RT images, the RR-interval was computed from the ED to ES distance for each beat. It then served to calculate the heart volume/min and heart volume/beat.

Segmentation of 3 T RT images was accomplished with use of the prototype software CaFuR (Fraunhofer Mevis, Bremen, Germany, Version 1.1) as shown in Fig. 2. This software is able to process large datasets with up to 600 images per plane. Left endo- and epicardial segmentation is done automatically based on polar scanning in all relevant slices and time points [17]. Nevertheless, in order to achieve a segmentation quality of RT images with CaFur which is similar to that of CINE images with QMass, every frame had to be inspected for eventual manual correction. Papillary muscles were assigned to the blood pool.

2.5. Statistical analysis

Statistical analysis was conducted using Microsoft Excel and IMB SPSS Statistics version 22 for Windows. Mean values and standard deviations (SDs) among patients were calculated for all measurements. Normality was tested using the Shapiro–Wilk test. Correlation (r) of parameters obtained from RT and CINE images were determined applying Pearson correlation and considered significant for p-value < 0.05. The level of correlation was defined as: good for $r \geq 0.5$, fair for $r \geq 0.3$, and poor for ≥ 0.1 [18]. Inter- and intra-observer agreement was tested by calculating mean bias and 95% limits of agreement (confidence intervals) from Bland–Altman analyses [19], coefficient of variation (CV), and interclass correlation coefficient (ICC) [3]. A p-value of < 0.05 was considered statistically significant for the level of agreement [20]. For the calculation of significance in the qualitative evaluation a Wilcoxon-matched pairs test was applied. Again, a p-value < 0.05 was considered statistically significant.

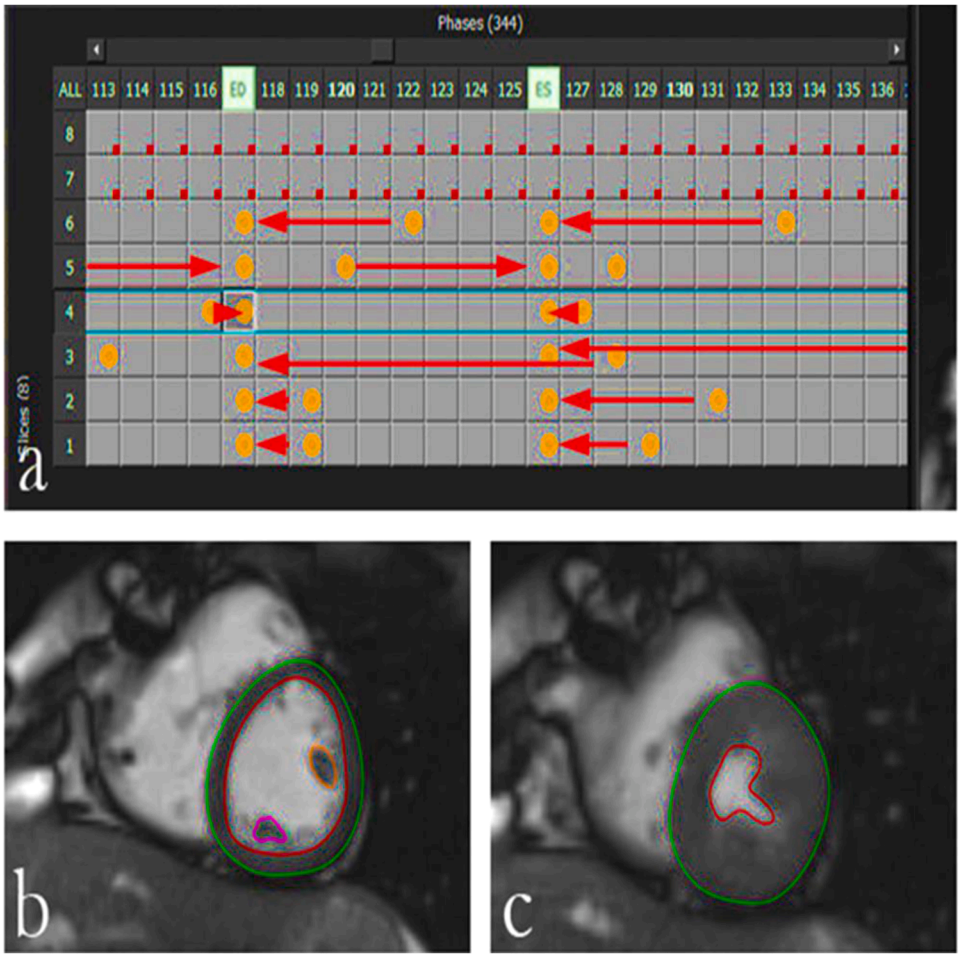

Fig. 1. Segmentation of 1.5 T RT SA images using QMass: (a) After segmentation all images were grouped into individual heart beats to generate a complete stack for further evaluation. Example: in row 6 the end-diastolic image is in column 122, this contour was copied to column 117 as were all other end-diastolic contours. The end-systolic contours were processed in the same way: e.g. row 6: contours in column 133 were copied and inserted in column 127. (b,c) Endocardial borders are shown in red and epicardial borders are shown in green in a mid-ventricular slice for end-diastolic (b) and end-systolic (c) frames. Papillary muscles are excluded from mass (orange and purple).

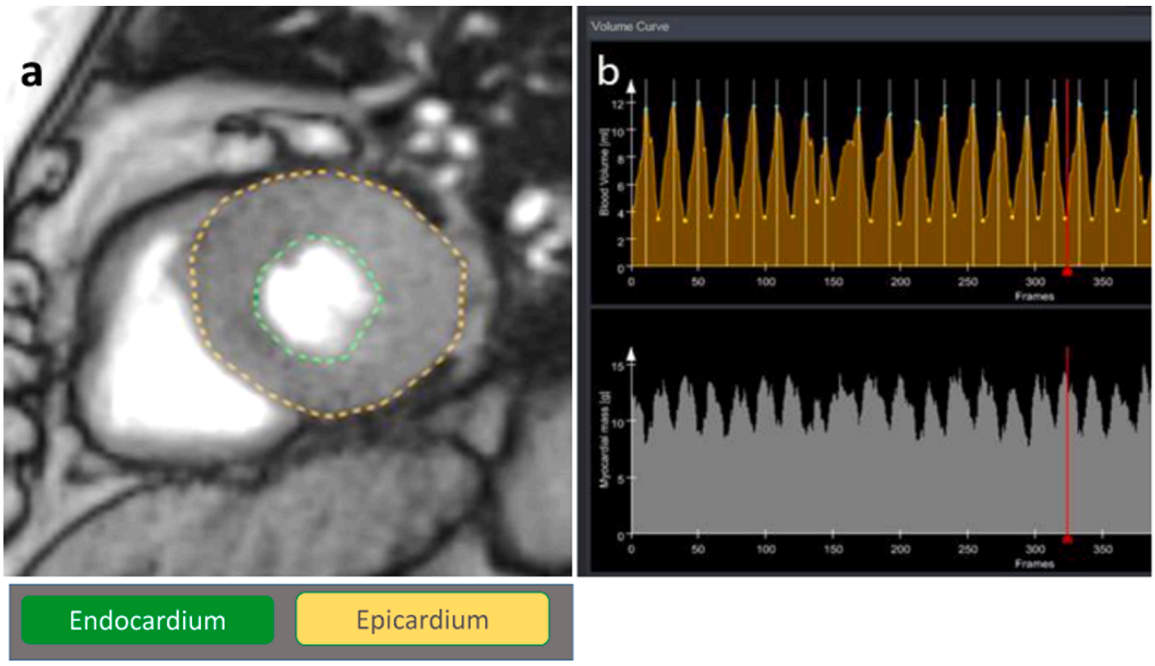

Fig. 2. Segmentation of 3 T RT SA images using CaFuR: (a) Automatic detection of endocardial (green) and epicardial borders (yellow). (b) Volumes (yellow volume curves, [ml]) and mass (white curves, [g]) for different cycles with maximal and minimal values representing end-diastolic and end-systolic volumes, respectively. The red line marks the position of the cardiac cycle depicted in (a).

3. Results

3.1. Image quality

3.1.1. Atrial fibrillation

Image quality was independently evaluated by two experienced observers. As summarized in Table 3 RT images at 1.5 T of arrhythmic patients had a significantly higher diagnostic quality compared to CINE images in all planes with the exception of the apical plane. As an example Fig. 3 shows mid-ventricular SA views from a patient with atrial fibrillation demonstrating significantly better image quality for RT CMR than for CINE CMR.

Similar results were obtained at 3 T as quantified (Table 3). The mean diagnostic quality in basal and mid-ventricular SA views was significantly better in RT images than in CINE images, examples are depicted in Fig. 4. At 3 T the improvement of image quality in RT CMR compared to CINE CMR was not significant in 2 C and 4 C views and in the apical short axis.

Quantification of mass, ED and ES volumes as well as EF require an accurate delineation of blood pool and endocardial and pericardial borders. Therefore, the observers also evaluated image quality of the anterior, inferior, septal and lateral wall as well as sharpness of the papillary muscles. Supplemental Digital Content 1 (Table 4) summarizes the scores for the septal and lateral wall in SA views for RT and CINE CMR. RT images are generally preferred for edge detection of cardiac structures in both patient cohorts. While the superior performance of RT CMR in arrhythmic patients was observed at both field strengths (Table 3 and Supplemental Content 1), the absolute scores were higher at 1.5 T than at 3 T. This also holds true for CINE images (Table 3).

3.1.2. Sinus rhythm

In control subjects both observers rated image quality higher for CINE acquisitions compared to RT CMR in all views, see Table 3. Nevertheless, real-time images of normal subjects were mostly considered to be of "good image quality with some artifacts" resulting in a good delineation of the wall and papillary muscles. Fig. 5 shows an example of a subject in two long-axis views: CINE CMR resulted in higher tissue contrast and thus better depicts the myocardium and papillary muscles. The lowest score was 2 (diagnostic quality with artifacts) given by both observers for RT CMR in three subjects.

3.1.3. Reproducibility

Qualitative results for the repeated analyses are summarized in Supplemental Digital Content 2. For the 1.5 T images observer 1 rated some CINE images better during the first reading, but overall the differences were not significant (data not given). The evaluation of 3 T images of patients with atrial fibrillation did not show a significant difference between the two readings for observer 1, while observer 2 evaluated apical images in the first reading significantly better than in the second reading. For images of control subjects in sinus rhythm (3 T)

Table 3
Image quality (mean ± SD) for RT and CINE CMR of patients (n = 59) with atrial fibrillation and controls (n = 20) at 1.5 and 3 T.

View	patients RT (1.5 T) n = 30	patients CINE (1.5 T) n = 30	p value	patients RT (3 T) n = 29	patients CINE (3 T) n = 29	p value	controls RT (3 T) n = 20	controls CINE (3 T) n = 20	p value
2 C	3.2 ± 0.6	2.65 ± 1.1	**0.011**	2.6 ± 0.85	2.45 ± 0.85	0.18	3.35 ± 0.4	3.9 ± 0.15	**< 0.001**
4 C	2.9 ± 0.65	2.4 ± 0.9	**0.0044**	2.55 ± 0.95	2.4 ± 1.0	0.65	3.35 ± 0.05	3.9 ± 0.25	**0.045**
SA basal	3.5 ± 0.5	2.55 ± 0.8	**0.0003**	2.85 ± 1.0	2.4 ± 0.9	**0.04**	3.0 ± 0.5	3.8 ± 0.45	**0.03**
SA mid	3.55 ± 0.5	2.6 ± 0.9	**0.0001**	3.15 ± 0.9	2.6 ± 1.0	**0.03**	3.35 ± 0.45	3.8 ± 0.5	**0.008**
SA apical	2.7 ± 0.8	2.75 ± 0.75	0.357	2.7 ± 1.05	2.3 ± 0.85	0.14	3.0 ± 0.6	3.85 ± 0.4	**0.002**

$p < 0.05$ significant difference

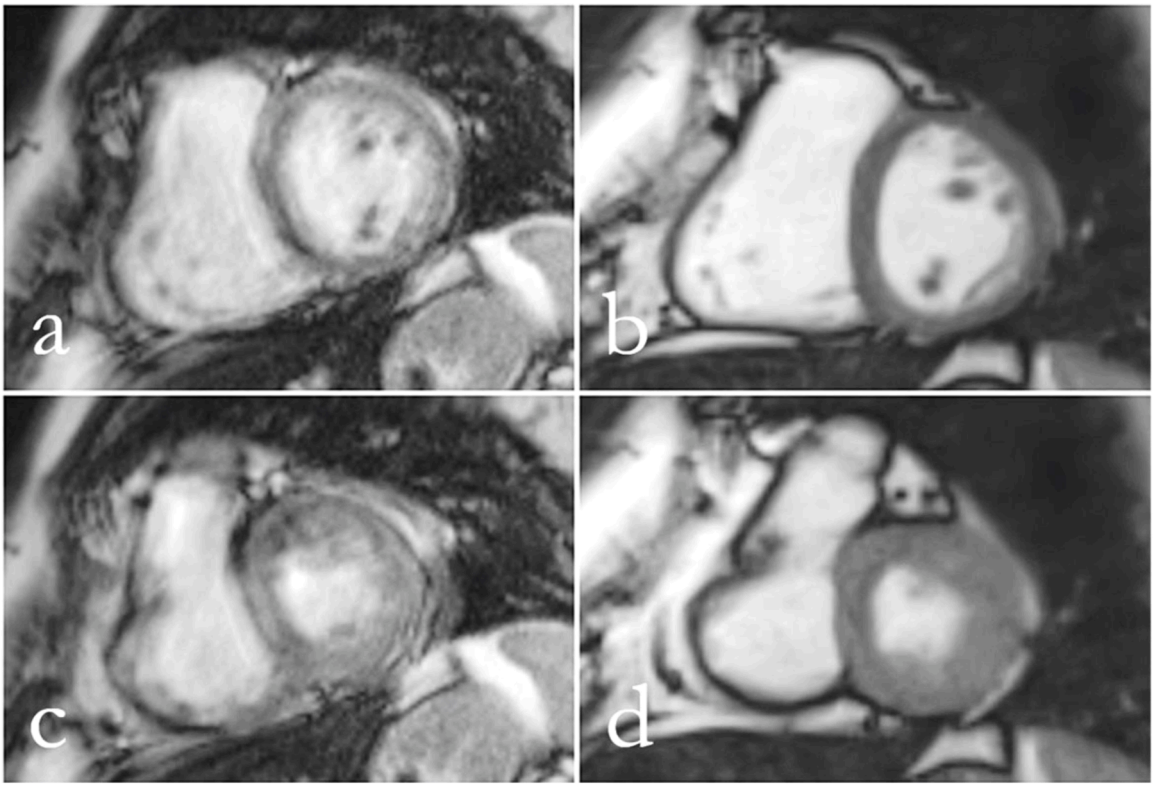

Fig. 3. (a,c) CINE and (b,d) RT CMR at 1.5 T of a patient with atrial fibrillation in a mid-ventricular SA view during end-diastole (a,b) and end-systole (c,d). CINE mages have reduced diagnostic quality (score 1), while RT images present with good diagnostic quality (score 4).

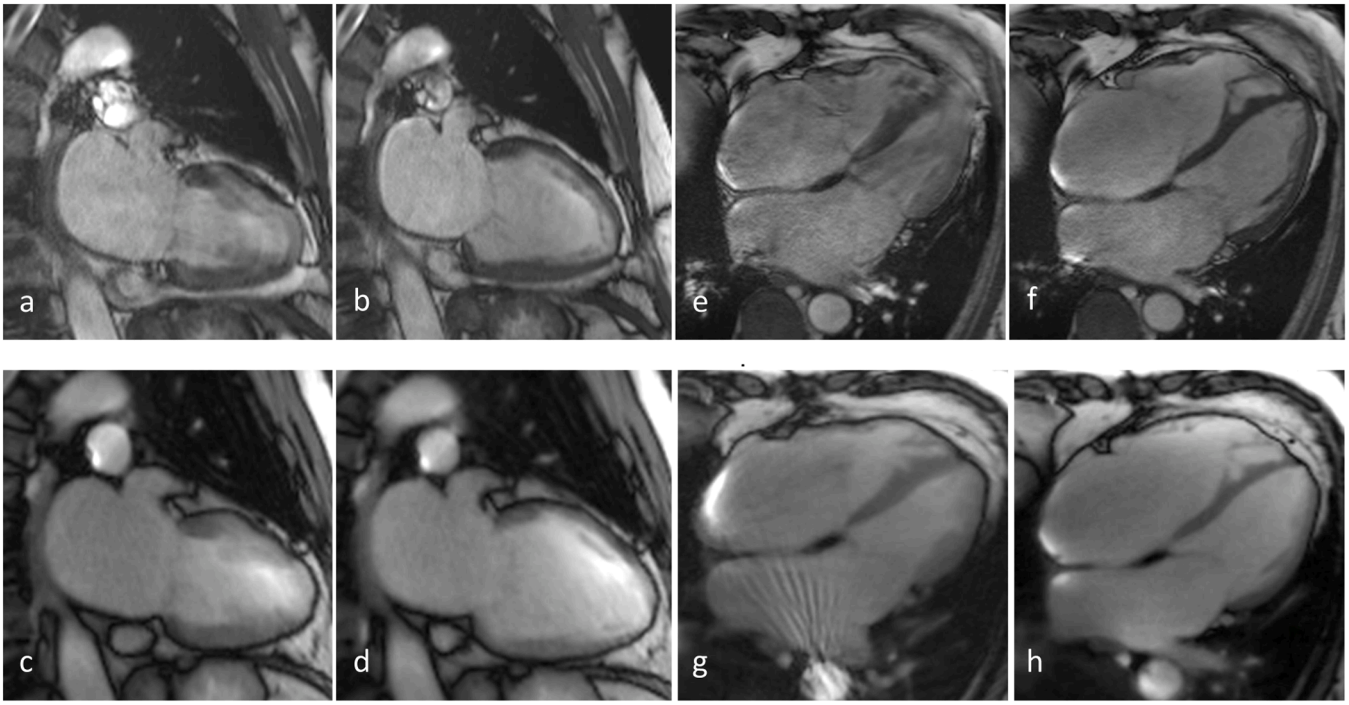

Fig. 4. (Top) CINE and (bottom) RT CMR at 3 T of a patient with atrial fibrillation in a 2 C and 4 C view, respectively. The frames refer to end-systole (a,c,e,g) and end-diastole (b,d,f,h). RT images (4 C view) reveal good quality (score 3), while CINE images exhibit reduced quality (score 2). (g) bSSFP banding artifact causing streaks.

there was no significant difference for both readings and both observers.

For 3 T acquisitions the intra-observer agreement for all RT and CINE quantitative parameters in all patients and controls were highly correlated ($p < 0.001$); RT patients: average CV = 3%; RT controls: average CV= 2.6%; CINE patients: average CV= 1.6%; CINE controls: average CV = 1.6%. The inter-observer agreement showed a high level

Table 4
Left-ventricular data (mean ± SD) for 3 T RT and CINE CMR in patients with atrial fibrillation (n = 29) and controls (n = 20).

Patients	RT	CINE	r	p value
ESV [ml]	94 ± 52	106 ± 55	0.921	< 0.001
ESV-index [ml/m²]	46 ± 22	52 ± 24		
EDV [ml]	172 ± 68	185 ± 66	0.902	< 0.001
EDV-index [ml/m²]	86 ± 29	93 ± 29		
SV [ml]	82 ± 29	79 ± 26	0.756	< 0.001
SV-index [ml/m²]	42 ± 14	41 ± 15		
EF [%]	47 ± 16	45 ± 13	0.679	< 0.001
MM [g]	128 ± 42	135 ± 39	0.878	< 0.001
MM-index [g/m2]	66 ± 29	69 ± 21		
Controls				
ESV [ml]	56 ± 16	61 ± 14	0.708	< 0.001
ESV-index [ml/m²]	31 ± 7	33 ± 6		
EDV [ml]	151 ± 33	163 ± 36	0.879	< 0.001
EDV-index [ml/m²]	83 ± 13	90 ± 14		
SV [ml]	95 ± 22	101 ± 27	0.944	< 0.001
SV-Index [ml/m²]	52 ± 9	56 ± 11		
EF [%]	63 ± 6	63 ± 3	0.695	< 0.001
MM [g]	93 ± 20	95 ± 25	0.898	< 0.001
MM-Index [g/m²]	51 ± 8	52 ± 10		

Pearson correlation (r) and p < 0.001 significant difference

of reproducibility ($p \leq 0.005$) as well; RT patients: average CV = 3.8%; RT controls: average CV = 4.6%; CINE patients: average CV = 5.6%; CINE controls: average CV = 4%. There were no notable differences in reproducibility for the analyses of RT and CINE CMR, neither in patients nor in healthy subjects.

3.2. Volumetry

Quantitative analyses were successfully performed in all 29 patients with atrial fibrillation and 20 control subjects with sinus rhythm at 3 T. While CINE images were analyzed with QMass, RT images were segmented using CaFur. For an experienced observer LV segmentation in patients takes about 8–10 min even with less sharp CINE contours. On the other hand, segmentation of all contours for a particular RT CMR dataset in QMass took about 120–150 min. As segmentation in CaFur with around 120 images per slice took about 45 min for a SA-stack we chose this software for the 3 T patients. Unfortunately CINE data cannot be loaded into the CaFur software.

The results in Table 4 show good to very good Pearson correlation (> 0.679) between RT and CINE CMR with high significance in all parameters ($p \leq 0.001$) for both patients and controls. In patients, the mean values for EDV, ESV and MM were slightly lower for RT CMR (ESV = 94 ± 52 ml, EDV = 172 ± 68 ml) in comparison to CINE CMR (ESV= 106 ± 55 ml, EDV = 185 ± 66 ml). In contrast, the mean EF was slightly higher in RT CMR (48% ± 16%) than obtained for CINE CMR (45% ± 13%). In controls mean values for EF in RT and CINE CMR were identical (63%), while other parameters revealed slightly higher values for CINE CMR.

As shown in the Bland-Altman-analysis in Supplemental Content 3 and Fig. 6 there is some bias between RT and CINE measurements for EDV (−12.36%) and ESV (−4.5%) in control subjects, but not for the EF (0.04%). In patients with atrial fibrillation bias was higher for all values compared to controls. Again the volumes were slightly lower in RT CMR compared to CINE CMR (ESV −12.4%, EDV −13.2%). Similar results were obtained in the 1.5 T patient group where RT and CINE images (SA views only) were both analyzed by QMass. Because the evaluation was restricted to images that allowed contour detection (score > 1), only 25 of the 30 patients at 1.5 T were included. Bland-Altman analysis of EF showed that CINE vs RT data resulted in a small bias of + 2% (limits −15% and 19%) with lower values for EDV, ESV, MM and SV in RT CMR.

4. Discussion

4.1. Image quality

Our results demonstrate that free-breathing RT CMR based on undersampled radial bSSFP acquisition and NLINV reconstruction [11, 13] improves image quality in patients with atrial fibrillation compared to conventional ECG-synchronized CINE imaging. This improvement was significant for scans at 1.5 T and at 3 T (basal and mid-ventricular

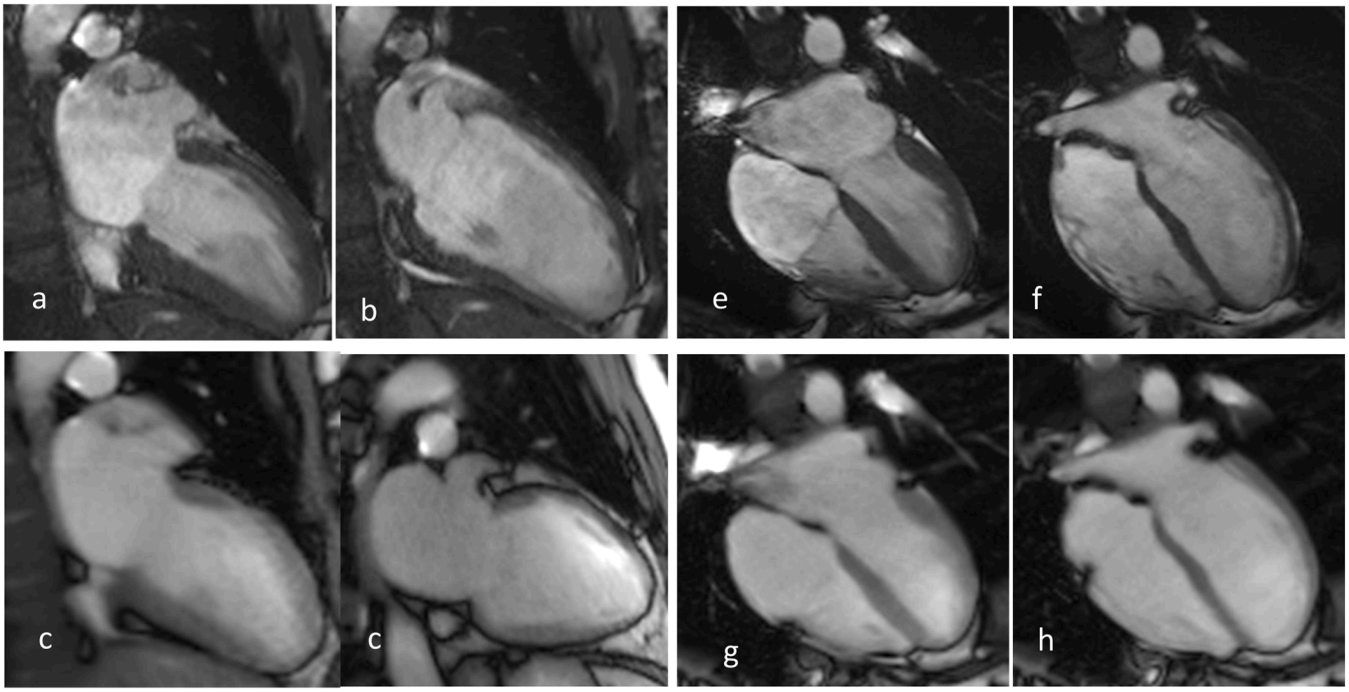

Fig. 5. (Top) CINE and (bottom) RT CMR at 3 T of a healthy subject in sinus rhythm in a 2 C and 4 C view, respectively. The frames refer to end-systole (a,c,e,g) and end-diastole (b,d,f,h).

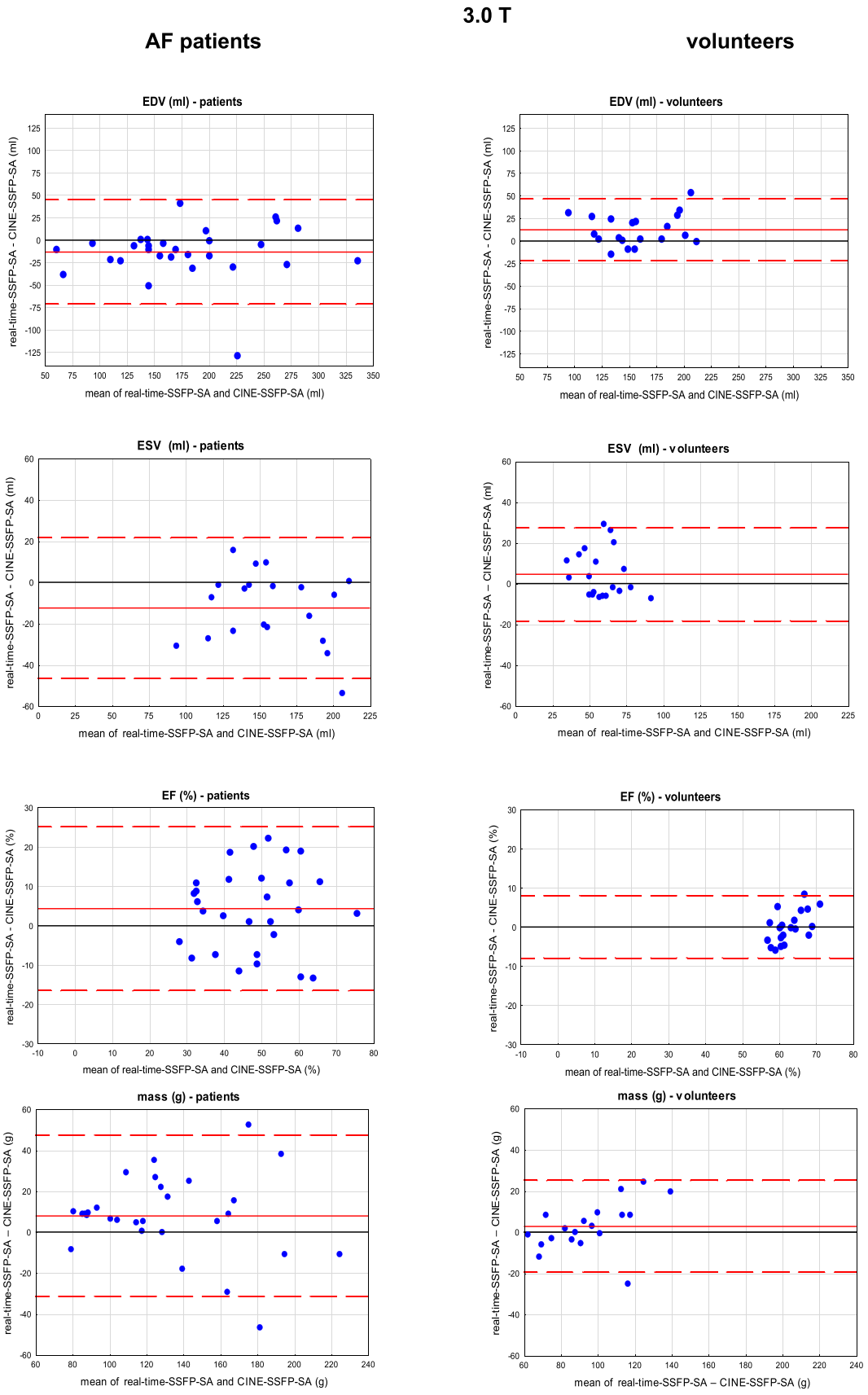

Fig. 6. Bland-Altman plots (RT vs CINE) of ejection fraction (EF), end-diastolic volume (EDV), end-systolic volume (ESV), and myocardial mass in patients with atrial fibrillation (3 T and 1.5 T) and controls (3 T) with mean difference (red line) and limits of agreement (1.96 SD, red dotted lines).

SA). The only exception in the short axis were apical planes with a tendency for higher quality in RT CMR. Apical planes pose problems in general correspondingly in RT CMR as the small lumen and the high amount of trabeculae complicate the delineation of contours. These findings confirm our previous 1.5 T study [12] now in a larger cohort of arrhythmic patients and reassure that the quality of CINE images is often insufficient for arrhythmic heart beats (mainly due to blurring and motion artifacts), whereas image quality is substantially improved by RT CMR. Similar improvements in image quality for arrhythmic patients were reported for accelerated MRI techniques based on parallel imaging with compressed sensing for both 1.5 T [25,26] and 3 T [27]. However, these techniques do not fully qualify as real-time imaging as the requirement for temporal sparsity only allows for image reconstructions after completion of the entire dynamic data acquisition.

For subjects with regular (sinus) rhythm RT CMR was inferior compared to CINE CMR mainly due to residual streaking artifacts from radial undersampling [22,23]. In addition, the advantage of a higher field strength could not be fully realized with RT CMR when using bSSFP sequences: firstly, this is because short repetition times preclude the use of a flip angle as high as usually employed for CINE CMR. However, initial tests indicate that the blood-myocardium contrast may be improved when higher flip angles are realized at the expense of longer RF pulses, which slightly reduces the number of radial spokes per frame but does not affect the temporal resolution. Secondly, for RT CMR the tissue contrast is eventually reduced during systolic contraction as RT acquisitions reflect the accompanying through-plane motion of the heart along its long axis. This effect reduces any T1 saturation and/or partially spoils the bSSFP signal, a problem also observed for other acceleration techniques [24]. Despite these restrictions, the quality of RT bSSFP CMR was considered high enough for a volumetric analysis and diagnostic evaluation of wall motion. Whether the use of T1-weighted sequences for 3 T RT CMR offers further improvements remains to be seen [24]. Moreover, minor quality values were observed at 3 T compared to 1.5 T images independent on the scanning mode. This might be due to off-resonance and flow artifacts present in both RT and CINE images as a typical consequence of bSSFP sequences at 3 T [21].

4.2. Volumes and function

With respect to cardiac volumes and ejection fraction, there is no statistically significant difference between RT and CINE CMR in controls with sinus rhythm despite a tendency towards smaller volumes in RT CMR compared to CINE CMR.

For the 1.5 T study RT and CINE images were both analyzed using Medis QMass. As this software cannot automatically sort RT images into ED and ES frames, this task had to be accomplished manually which is highly time-consuming and not practicable in clinical routine. Moreover, this approach merges data from different cardiac cycles with varying length into a single heartbeat and thus loses the advantage of RT CMR, i.e. access to individual heartbeats. Therefore, the prototype software CaFur which allows for a semiautomatic function analysis of multiple heartbeats was applied to analyze the 3 T RT CMR data. The program full-automatically inserts endocardial and epicardial contours in all images with the option to perform manual corrections. This technique opens the possibility to analyze the functional variability of heart beats in patients with arrhythmia [28]. In our hands time for image analysis using CaFur could be reduced by a factor of > 2.6 compared to Medi Q Mass.

A comparison of RT CMR analyses by CaFur CINE with CMR analyses by QMass showed significant agreement, regardless of cardiac rhythm. There was a tendency for lower ED and ES volumes for RT vs CINE CMR. Both programs showed good inter- and intra-observer reproducibility. Nevertheless, individual functional values in patients with atrial fibrillation revealed relevant discrepancies. One possible explanation is that RT CMR values in arrhythmic patients are closer to true volumes. In fact, the analysis of multiple individual heartbeats takes into account any arrhythmia-induced variations of cardiac movements and functions including shorter cycles. On the other hand, established algorithms for reconstructing CINE CMR datasets might be biased toward longer cardiac cycles in order to provide a minimum number of, for example, 25 frames. Such strategies implicitly discard shorter (aperiodic) beats which likely to lead to a less expanded myocardium and thus lower volumes. A related observation was reported by Goebel et al. [25] who applied a different software for a volumetric analysis of compressed sensing reconstructions where volumes of accelerated images were lower than those obtained by CINE imaging. Further reasons for functional differences may possibly originate from differences in analysis software and respective algorithms for contour tracking.

Finally, at this stage, the used RT CMR technique only allows for cross-sectional imaging. Thus, in order to cover the entire heart, it was necessary to sequentially determine a stack of RT CMR movies as it is done in CINE. This problem may be possibly overcome by simultaneous multi-slice real-time MRI [29].

5. Limitations

A limitation of our study is that image quality is a subjective measure. Both observers evaluated independently, blinded and randomwise. However, as RT and CINE CMR are inherently different (typical tissue contrast), blinding was not effective and may lead to a scoring bias. Bias between readers was indeed detectable in the 1.5 T study but was not observed at 3 T. Volumetric analysis of RT images in QMASS software is time consuming Therefore the alternative software CaFuR for analysis of large amounts of images was applied for the RT images in 3 T. Differences in values between CINE and RT for the 3 T groups might be partly due to the use of these two softwares.

6. Conclusion

Our findings demonstrate that, based on bSSFP sequences, RT CMR improves image quality in arrhythmic patients with atrial fibrillation compared to CINE acquisitions at both 1.5 T and 3 T field strength. During regular (sinus) rhythm RT CMR has less image quality compared to CINE CMR but still yields diagnostic quality. It may therefore be exploited for shortened exams without the need for breath-holding. Volumetric analyses are feasible, while different reconstruction and analysis techniques for RT and CINE CMR may contribute to slightly smaller volumes. Because of its nature as a difference value, ejection fractions turned out to be comparable independent of acquisition and analysis. In future, there is an urgent need for advanced analysis software with optimized automatic contour detection, faster processing for large datasets either in RT or CINE CMR.

Ethics approval and consent to participate

The study was approved by the local ethic committee. Written informed consent was obtained from each participant before the study.

Funding

The work was partially supported by the German Centre for Cardiovascular Research Project number 81Z0300115 partner site Goettingen (DZHK).

Authors' contributions

KL experimental analysis, interpretation of data and writing of manuscript; TvL experimental workup, analysis and interpretation of data; CR critical revision of manuscript; MS critical revision of the manuscript; JL critical revision of the manuscript; DV development of real-time MRI methods; JF development of real-time MRI methods and critical revision of manuscript; MU development of real-time MRI

methods, data collection and analysis and drafting the manuscript; CUB conception, design of the study, experimental workup, analysis and interpretation of data and writing of manuscript. All authors read and approved the final manuscript.

Acknowledgements

We are particularly grateful for the assistance given by Ulrike Köchermann and Tanja Otto.

Declarations

All authors hereby disclose any financial and personale relationship with other people or organizations that could inappropriately influence or bias their work.

Consent for publication

Consent for publication was obtained from all participants in the study.

Competing interests

JF and MU are co-inventors of a patent covering the real-time MRI technique used in this study. All other authors disclose any financial and personale relationship with other people or organizations that could inappropriately influence or bias their work.

Appendix A. Supporting information

Supplementary data associated with this article can be found in the online version at doi:10.1016/j.ejro.2022.100404.

References

[1] J.P. Curtis, S.I. Sokol, Y. Wang, et al., The association of left ventricular ejection fraction, mortality, and cause of death in stable outpatients with heart failure, Am. J. Coll. Cardiol. 42 (2003) 36–742.
[2] J.J. McMurray, S. Adamopoulos, S.D. Anker, et al., ESC committee for practice guidelines 2. ESC guidelines for the diagnosis and treatment of acute and chronic heart failure 2012: the task force for the diagnosis and treatment of acute and chronic heart failure 2012 of the European Society of Cardiology. Developed in collaboration with the Heart Failure Association (HFA) of the ESC, Eur. J. Heart Fail 14 (8) (2012) 803–869.
[3] F. Grothues, G.C. Smith, J.C. Moon, et al., Comparison of interstudy reproducibility of cardiovascular magnetic resonance with two-dimensional echocardiography in normal subjects and in patients with heart failure or left venricular hypertrophy, Am. J. Cardiol. 90 (2002) 29–34.
[4] D. Saloner, J. Liu, H. Haraldsson, MR physics in practice: how to optimize acquisition quality and time for cardiac MR imaging, Magn. Reson. Imaging Clin. N. Am. 23 (2015) 1–6.
[5] P.F. Ferreira, P.D. Gatehouse, R.H. Mohiaddin, et al., Cardiovasc magnetic resonance artefacts, J. Cardiovasc. Magn. Reso. 22 (2013) 15–41.
[6] K.T. Block, M. Uecker, J. Frahm, Undersampled radial MRI with multiple coils. Iterative image reconstruction using a total variation constraint, Magn. Reson. Med. 57 (2007) 1086–1098.
[7] M. Lustig, D. Donoho, J.M. Pauly, Sparse MRI: The application of compressed sensing for rapid MR imaging, Magn. Reson. Med. 58 (2007) 1182–1195.
[8] M. Uecker, T. Hohage, K.T. Block, et al., Image reconstruction by regularized nonlinear inversion – joint estimation of coil sensitivities and image content, Magn. Reson. Med. 60 (2008) 674–682.
[9] N. Seiberlich, P. Ehses, J. Duerk, et al., Improved radial GRAPPA calibration for real-time free-breathing cardiac imaging, Magn. Reson. Med. 65 (2011) 492–505.
[10] M. Uecker, S. Zhang, J. Frahm, Nonlinear inverse reconstruction for real-time MRI of the human heart using undersampled radial FLASH, Magn. Reson. Med. 2010 (63) (2010) 1456–1462.
[11] Uecker M. , Zhang S. , Voit D. Karaus A. , et al., 2010. Real-time MRI at a resolution of 20 ms NMR Biomed. 2010; 23: 986–994.
[12] S. Zhang, M. Uecker, D. Voit, et al., Real-time cardiovascular magnetic resonance at high temporal resolution: radial FLASH with nonlinear inverse reconstruction, J. Cardiovasc. Magn. Reson. 12 (2010) 39.
[13] S. Voit, Zhang, C. Unterberg-Buchwald, et al., Real-time cardiovascular magnetic resonance at 1.5 T using balanced SSFP and 40 ms resolution, J. Cardiovasc. Magn. Reson. 15 (2013) 79.
[14] R. Likert, A technique for the measurement of attitudes, Arch. Psychol. 22 (140) (1932) 55.
[15] Geest, R.J. van der , 2011. Automated image analysis techniques for cardiovascular magnetic resonance imaging. Doctoral thesis, Leiden University. ISBN: 9789490858049. ⟨http://hdl.handel.net/1887/16643⟩.
[16] J. Schulz-Menger, D.A. Bluemke, J. Bremerich, et al., Standardized image interpretation and post processing in cardiovascular magnetic resonance: Society for Cardiovascular Magnetic Resonance (SCMR) board of trustees task force on standardized post processing, J. Cardiovasc. Magn. Reson. 15 (2013) 35.
[17] Zoehrer F., Huellebrand M., Chitiboi T., et al. Real-time myocardium segmentation for the assessment of cardiac function variation. In A. Krol, & B. Gimi (Eds.) Medical Imaging 2017: Biomedical Applications in Molecular, Structural, and Functional Imaging. 2017; 10137: 101370L.
[18] L.M. Cohen, P.J. Koltai, J.R. Scott, Lateral cervical radiographs and adenoid size: do they correlate? Ear. Nose Throat. J. 71 (1992) 638–642.
[19] J.M. Bland, D.G. Altman, Measuring agreement in method comparison studies, Stat. Methods. Med. Res. 8 (1999) 135–160.
[20] K. Oppo, E. Leen, W.J. Angerson, et al., Doppler perfusion index: an interobserver and intraobserver reproducibility study, Radiology 208 (1998) 453–457.
[21] P. Rajiah, M.A. Bolen, Cardiovascular MR imaging at 3 T: opportunities, challenges, and solutions, Radiographics 34 (2014) 1612–1635.
[22] Block KT, Uecker M., Frahm J. Undersampled radial MRI with multiple coils. Iterative image reconstruction using a total variation constraint. J Magn Reson Med. 57, 1086–1098.
[23] H. Haji-Valizadeh, A.A. Rahsepar, J.D. Collins, et al., Optimal Management with Binders and NicotinamidE (COMBINE) Study Group. Validation of highly accelerated real-time cardiac CINE MRI with radial k-space sampling and compressed sensing in patients at 1.5T and 3T, Magn. Reson. Med. 79 (2018) 2745–2751.
[24] S. Zhang, A.A. Joseph, D. Voit, S. Schaetz, K.D. Merboldt, C. Unterberg-Buchwald, A. Hennemuth, J. Lotz, J. Frahm, Real-time MRI of cardiac function and flow – Recent progress, Quant. Imaging Med. Surg. 4 (2014) 313–329.
[25] J. Goebel, F. Nensa, H.P. Schemuth, et al., Compressed sensing CINE imaging with high spatial or high temporal resolution for analysis of left ventricular function, J. Magn. Reson. Imaging 44 (2016) 366–374.
[26] B.A. Allen, M.L. Carr, M. Markl, et al., Accelerated real-time cardiac MRI using interactive sparse SENSE reconstruction: comparing performance in patients with sinus rhythm and atrial fibrillation, Eur. Radiol. 28 (2018) 3088–3096.
[27] S. Sudarski, T. Henzler, H. Haubenreisser, et al., Free-breathing sparse sampling CINE MR imaging with iterative reconstruction for the assessment of left ventricular function and mass at 3.0 T, Radiology 282 (2017) 74–83.
[28] L. Wang, T. Chitiboi, H. Meine, M. Gunther, H.K. Hahn, Principles and methods for automatic and semi-automatic tissue segmentation in MRI data, MAGMA 29 (2016) 95–110.
[29] S. Rosenzweig, H.C.M. Holme, R.N. Wilke, D. Voit, J. Frahm, M. Uecker, Simultaneous multi-slice reconstruction using regularized nonlinear inversion: SMS-NLINV, Magn. Reson. Med. 79 (2018) 2057–2066.